Reaction front characterization in turbulent combustion based on entropy production field curvature

R. Schießl, V. Bykov
Institut für Technische Thermodynamik
Karlsruher Institut für Technologie (KIT)

1 Introduction

The mathematical modeling and numerical investigation of turbulent combustion phenomena represents very complicated fields of combustion theory and applications [1,2]. There is increasing activity towards numerical investigations of turbulent flames using Direct Numerical Simulations (DNS) [3]. From an application point of view, non-premixed turbulent combustion system is of primary importance. In order to study properties of this combustion system there is a standard approach to trace the reaction flame front by using mixture fraction (around stoichiometric values) [2]. Then, properties of the system (such as species profiles, heat release, flame structure etc.) are investigated and represented in a local coordinate frame attached to iso-surfaces of constant mixture fraction. Various combustion models (like e.g. the Schmidt model, flamelets, FGM and related concepts) rely on this concept. While this has successfully been used for the prediction of combustion in many cases, it might lead to inaccurate predictions when e.g. local extinction or re-ignition take place. Research for alternative concepts to identify the flame front as a basis for the development of reliable combustion sub-models is still active [3,4,5].

In our work, the chemical entropy production rate (CEPR) is suggested as a marker for chemical reaction. The reaction front and its geometrical structure are described by local eigenspaces of the Hessian (matrix of second spatial derivatives) of the entropy production term computed in the physical space. Moreover, eigenvalues can be used to study geometry and dimensionality of the reaction front, while local eigenspaces and path-following algorithm can be used to trace the flame front and represent the data in the physically appropriate local coordinate frame. The method was implemented to DNS of a turbulent, non-premixed hydrogen/air flame. It is found, in particular, that the reaction front at some locations is not a two-dimensional surface, but rather has characteristics of a one-dimensional, filament-like structure. This observation can be used, for instance, to more accurately quantify an effective flame surface of a turbulent flame, and therefore, for improved models of the flame propagation velocity in turbulent combustion. The exact relation of these filament-like structures to turbulence-chemistry interaction, as well as to other one-dimensional turbulence structures, still needs to be investigated.

Correspondence to: robert.schiessl@kit.edu

2 Methodology

DNS-Data: DNS simulations of a turbulent non-premixed planar flame at atmospheric pressure, where nitrogen-diluted hydrogen (75/25 N_2/H_2 by mole) flows counter an air stream (79/21 N_2/O_2 by mole), both at 298 K, are used for the study. The DNS were performed at ISUT, Magdeburg University, by their highly parallel, three-dimensional code DINOSOARS [6], a low Mach number solver using a 6th order finite difference scheme for spatial derivatives and a 4th order explicit Runge-Kutta scheme for time integration. All kinetic and transport properties were handled using Cantera 1.8 and Eglib 3.4 [7]. The detailed chemistry scheme of [8] for the oxidation of hydrogen was used to evaluate the chemical source term. This mechanism was chosen because it has been used and tested in our group now for a lot of cases; it also has been validated with different new mechanisms (e.g., Boivin et al. [9]), and with experimental data. The computational domain is a rectangular cuboid with a size of $1\times1.2\times1$ cm^3 , discretized over 384×513×384 equidistant grid points, respectively. The DNS are initialized with species- and temperature profiles from a laminar one-dimensional flame simulation, which are then extended along the 3D-geometry. In the 3D-DNS, the boundary conditions in y-direction were outlet-outlet, while periodic boundary conditions are chosen for x- and z-directions. A velocity field corresponding to artificial turbulence, with a Taylor Reynolds number Re_λ=60, large eddy turn-over time τ_Λ = 0.48 ms, fluctuation u′ = 2.8 m/s and integral length scale Λ = 1.35 mm is then overlaid. The Kolmogorov length (51.4 μm) and time scales (70.3 μs) are fully resolved in the DNS simulation. An adaptive time step based on CFL and Fourier number was used, with an average step size of 30 ns.

***Data Analysis*:** A reaction front is identified in the DNS data as a post-processing step. Several scalars could be employed as reaction front markers, e.g., the chemical source term of some species, or the heat release rate (HRR). However, a single specie's source term does not monitor the overall chemical activity, and the magnitude of the HRR can be small even in presence of strong chemical activity (the effects of exothermic and endothermic reactions may cancel); moreover, HRR can be negative or positive. A quantity that is positive for any chemical activity in a combustion system is the rate of chemical entropy production; the second law of thermodynamics guarantees this positivity. We used this field in our analysis. Therefore, first the mass-specific chemical entropy production rate (CEPR, in W/(kg·K)) ω_s was computed for every spatial point in the DNS data set. For an isobaric, reacting system, the CEPR is computed as:

$$\omega_S = \sum_{i=1}^{N} \omega_{Y_i} s_i + c_p \frac{\omega_T}{T} .$$

With index *i* running from 1 to the number of chemical species *N*, ω_{Y_i} denotes the chemical source term in a mass-fraction scale and s_i denotes the specific entropy, respectively, of species *i*. c_p is the specific heat capacity at constant pressure of the mixture, *T* its temperature, and ω_T the temporal rate of temperature change induced by chemical reaction. c_p and s_i are temperature- and composition dependent. The chemical source terms were computed from the species mass fractions, temperature and pressure using the same reaction mechanism and thermodynamic data that had also been used in the preceding DNS calculations.
For illustration, various scalar fields, including ω_s, from a sample DNS data set are depicted in Fig.1, in form of 2D slices cut out of the 3D data set. For instance, OH mass fraction (Y_OH) can be large in regions where the local reaction activity is practically zero (e.g., near the right edge of the frames in Fig. 1). The appearance of the ω_s field roughly matches the heat release (not shown here); local differences exist, however. Like the heat release, the CEPR can be used with both premixed and non-premixed combustion.

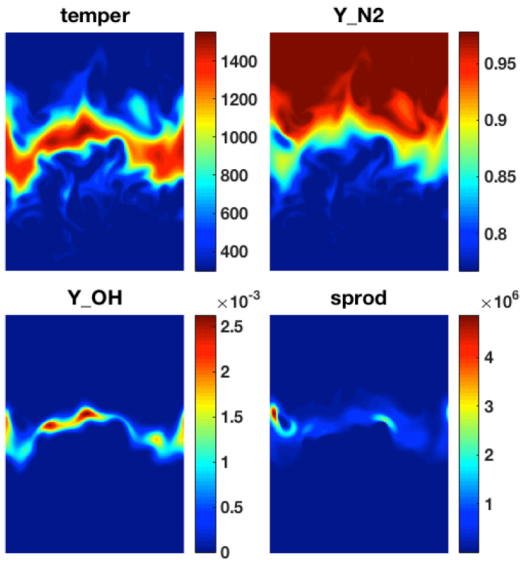

Figure 1: Planar 2D-slices through different instantaneous scalar fields from the DNS data set. The size of the scene is 1 cm × 1.2 cm.

The resulting CEPR field served as the basis for a subsequent reaction field analysis. To identify and track the reaction structure numerically, the following procedure was used:
First, a local maximum of the CEPR-field was identified. The local Hessian **H** (the matrix of second spatial derivatives) of CEPR was then determined at this local maximum. **H** is a real-valued, symmetric matrix, which contains information about the curvature of the ω_S-field in three-dimensional space.

The local structure of the reaction field can be characterized by an eigenvalue decomposition of the Hessian.

$$\mathbf{H} = \mathbf{A}\Sigma\mathbf{A}^{-1} \qquad (1)$$

where **A** is a 3×3 matrix containing eigenvectors as columns, and $\sum$ is a 3×3 diagonal matrix of eigenvalues, i.e., $\sum$ and **A** are of the form:

$$\Sigma = \begin{pmatrix} \sigma_1 & 0 & 0 \\ 0 & \sigma_2 & 0 \\ 0 & 0 & \sigma_3 \end{pmatrix}, \quad \mathbf{A} = \begin{pmatrix} \mathbf{u} & \mathbf{v} & \mathbf{w} \\ | & | & | \\ | & | & | \end{pmatrix}.$$

A is orthonormal because **H** is symmetric; therefore **u**, **v** and **w** form a rectangular coordinate frame. It points in the directions of the main curvatures of ω_S, and the corresponding eigenvalues characterize the "strength" of these curvatures. $\sum$ and **A** can be rendered into a form where the eigenvalues σ_i are arranged in order of decreasing magnitude along the diagonal; then, the eigenvector **u** corresponds to the strongest curvature (regardless of sign), eigenvector **w** to the weakest.

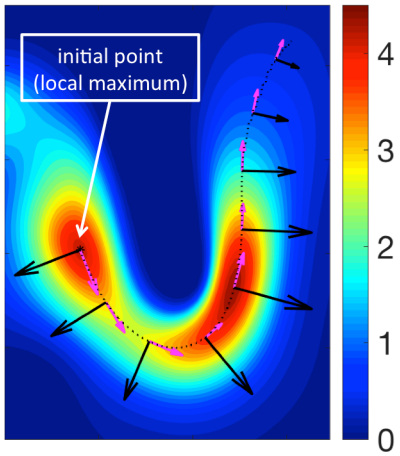

Figure 2: 2D ω_S field (1.7 mm × 2.5 mm) from the DNS (color contours in units of 10^6 W/(kg·K)); Black/magenta arrows are directions of strong/weak curvature, respectively. Lengths of vectors represent the magnitude of the corresponding eigenvalues. The black dotted line is the tracked reaction front.

The eigenvectors are used to obtain information about the local shape and orientation of the reaction structure. For this, a path-following algorithm is employed to track the reaction front from point to point.

For illustration, this is demonstrated on a 2D example in Fig. 2, which shows a 2D-cut out from the 3D DNS field ω_S as a false-color contour plot. First, an initial spatial point **x** is selected at a local maximum of the ω_s-field; this is a measure to ensure that the initial point is on the reaction structure. The Hessian and its eigenvalue decomposition at **x** are computed, which yields the direction of weakest curvature (eigenvector **w**). **x** is then updated to **x**=**x**+D**w**, where D is 1/4 of the DNS resolution (26 nm); note that **w** has length 1. The calculation of the local Hessian and its eigenvalue decomposition are then repeated at the new location in an iterative fashion. As a result, **x** follows, step by step, the local direction of the

eigenvector corresponding to least curvature. Some additional refinements are added to make the algorithm more robust:

- ensuring that the eigenvectors do not "flip" between points, i.e., do not point to the opposite half-space compared to the previous step. Flips can occur numerically because the sign of the eigenvectors in the decomposition (1) is arbitrary.
- slightly shifting x along the direction of the strong-curvature eigenvector after some steps to correct for the discretization error caused by the finite stepsize algorithm. This is done by moving x to the next local extremum of the ω_S field along the direction of the strong curvature eigenvector.

The significance of the resulting path can be understood as follows: If the ω_S-field is interpreted as a relief (height) map, point **x** follows, starting at a mountain's top, the mountain ridge: High curvature prevails in a direction perpendicular to the ridge, while lower curvature prevails along (parallel to) the ridge. It terms of combustion; this can be interpreted as tracking the reaction front (the "ridge" of the ω_s field).

In two dimensions, there are two curvature magnitudes and associated directions. These directions, the eigenvectors of **H**, are drawn as arrows at selected points within the reaction zone in fig. 2. The arrows have been scaled by the magnitude of the corresponding eigenvalues; to make all vectors recognizable in the plot, this scaling is nonlinear (length is proportional to third root of eigenvalue). The black dotted line is the tracked reaction front. Evidently, the curvature along the first eigenvector is usually much higher than the one along the second eigenvector. The reaction front then is a coherent, band-like structure, and its local orientation is given by the second eigendirection (magenta-colored vectors), while the first eigendirection is perpendicular, "cuts through" the band.

The procedure outlined here can be applied also to three-dimensional fields; here there are three curvatures, and the possible reaction structures are more copious.

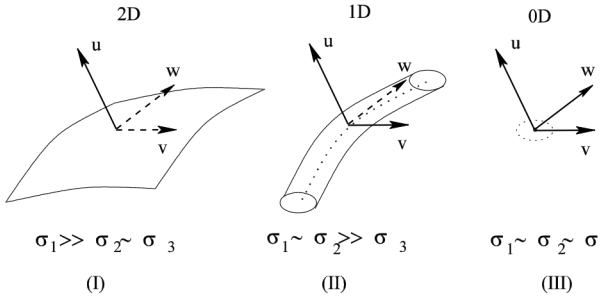

Figure 3: Classification of reaction field structures based on the subspaces associated with the main curvature directions.

Reaction front structure paradigms in three dimensions

In three dimensions, depending on the order of magnitude of the eigenvalues, one can sort out local directions of steepest entropy production gradients pointing in the direction of the flame propagation. Figure 3 highlights three typical cases for the flame front geometry: (I) one eigenvalue is dominant; (II) two eigenvalues are dominant over the third one; (III) all eigenvalues have the same order of magnitude.

These cases will define the local reaction field geometry by the corresponding co-dimension of the physical space. Thus, case (I) with one decoupled eigenvalue (only one dominant curvature) corresponds to a two-dimensional reaction front structure. There are two local spatial directions (**v,w**) in which there is weak (compared to the **u**-direction) curvature of the three-dimensional field. This is consistent with the notion of a classical two-dimensional flame sheet. The direction of the eigenvector corresponding to the dominant eigenvalue is the direction along which the CEPR-field has maximal curvature, while in the two other directions, no essential curvature is present.

Accordingly, when a maximum of entropy production is attained (the gradient becomes zero), the field can be characterized by the next-order derivative: Hessian can be used to investigate the local geometrical structure of the reaction front.

Thus, locally orthogonal eigenspaces can be used to distinguish and describe the local coordinate system that follows and represents the basis/directions in the physical state characterizing the chemical reaction front. The "strong" eigenvector is perpendicular to the local reaction sheet, the other two are tangential to the sheet. Case (II) with two decoupled eigenvalues features two spatial directions with strong curvature (two "strong" directions), while the third direction (the "weak" direction) exhibits only negligible curvature. This corresponds to a one-dimensional structure, appearing as a filamentary or "worm"-like object extending in direction given by the "weak" vector. The plane spanned by the two "strong" vectors (**u** and **v**) cuts perpendicularly through the filament. Finally, case (III) results in structures with no dominant direction of curvature at all, resulting in reaction "islands" with roughly spherical shape.

3 Results

Figure 4 shows a three-dimensional analog of the illustrative 2D-sample in Fig. 1. This is a typical result of a reaction front as identified and tracked in the DNS data using the method described above. Again, starting from a local maximum of the ω_s field, the direction of the smallest local curvature (eigenvector **w**) is followed. The path obtained this way is shown as a black curve. Note that the curve forms a closed loop; this is a feature that appeared quite frequently in the data set we studied. In the figure, some path-perpendicular planes (spanned by the local **u** and **v** vectors, see above) on which the local ω_s field is shown as a false-color plot, are drawn. This highlights the reaction field in the vicinity of the black curve, visually revealing a "worm"-like structure. Indeed, along the path shown, mostly paradigm (II) introduced above prevailed, and the tracked reaction structure is really filament- or "worm"-like. In the DNS data set that we studied, reaction structures of this "worm"-type are a common phenomenon. These structures, which might be termed flame worms or florms due to their characteristic appearance, likely result from a gradual decay of initially two-dimensional, flame-sheet like reaction structures of type (I), as present in the early time steps of the DNS simulation, into tube-like entities under the influence of the turbulent flow field.

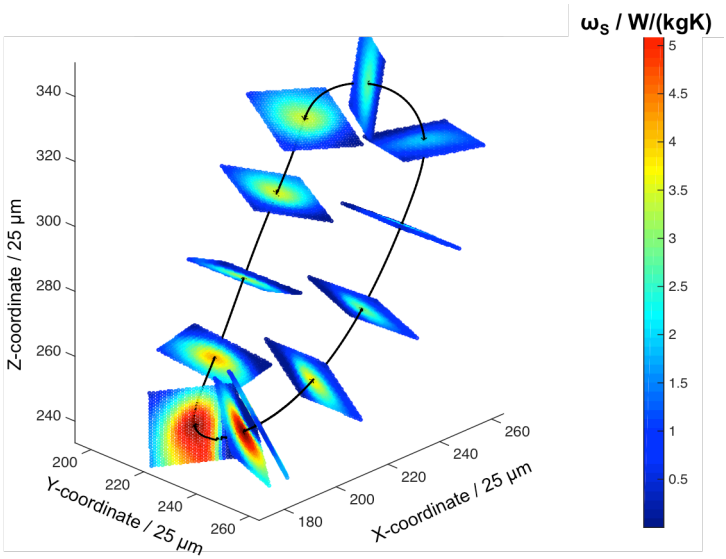

Figure 4: Sample of a reaction structure which is close to paradigm (II) (a flame worm or "florm") in the DNS data set. Black curve: Tracked path of reaction structure, obtained by following the local direction of the first eigenvector of the Hessian. Slices: local cut-outs (on planes spanned by the u and v eigenvectors of the Hessian) of the 3D field ω_S.

4 Conclusions

DNS data from a turbulent non-premixed diluted hydrogen/air flame were used to study geometrical characteristics of the turbulent reaction front. For this, it is proposed to use the chemical entropy production rate $\omega_{s.}$ as a universal marker for the reaction field. A characterization of reaction front geometry based on an eigenspace analysis of the local Hessian of the $\omega_{s.}$ field was introduced. In this way, natural locally orthogonal coordinate frame for statistical analysis of the turbulent flame can be obtained. This method allows a classification of local reaction field structures, and a distinction of structural paradigms (reaction "islands", "sheets" or "tubes"), depending on the magnitudes of the eigenvalues of the Hessian. In the studied dataset, "tube" or "worm"-like reaction structures were frequently observed. This classification may open alternative viewpoints on modeling of reaction-diffusion structures in highly turbulent flames. In the DNS data set we studied, structures of the "worm"-type could frequently be found. Typically, these flame "worms", which we propose to call *florms*, formed closed loops in space. The exact relation of the florms to turbulence-chemistry interaction, as well as to other one-dimensional turbulence structures, still needs to be investigated.

Acknowledgments

Financial support by the Deutsche Forschungsgemeinschaft (DFG) within TRR 150, TP B06 is gratefully acknowledged. The research group of Prof. Thevenin has kindly provided DNS data samples; their support is gratefully acknowledged.

References

[1] Warnatz J, Maas U, Dibble RW. (2004). Combustion , 4, Springer-Verlag, Berlin Heidelberg.

[2] Echekki, T., Mastorakos, E. (2011). Turbulent Combustion Modeling, Advances, New Trends and Perspectives, Springer-Verlag, Berlin, Heidelberg, New York.

[3] Chen J.H. (2011). Petascale direct numerical simulation of turbulent combustion – Fundamental insights towards predictive models, Proc. Combust. Inst. 33: 99.

[4] Lei Wang, Yong Jiang, Longwei Pan, Yu Xia, Rong Qiu. (2016). Lagrangian investigation and chemical explosive mode analysis of extinction and re-ignition in H2/CO/N2 syngas non-premixed flame, Int. J. of Hydrogen Energy. 41: 4820.

[5] Bennett, J.C., Krishnamoorthy, V., Liu, S., Grout, R.W., Hawkes, E.R., Chen, J.H., Shepherd, J., Pascucci, V., Bremer, P.-T. (2011). Feature-based statistical analysis of combustion simulation data, IEEE Transactions on Visualization and Computer Graphics 17: 1822.

[6] Abdelsamie, A., Fru, G., Oster, T., Dietzsch, F., Janiga, G., Thévenin D. (2016). Comput. Fluids 131: 123.

[7] A. Ern, V. Giovangigli. (1994). Multicomponent Transport Algorithms. Lecture Notes in Physics, New Series Monographs 24. Springer-Verlag, Heidelberg.

[8] U. Maas, J. Warnatz. (1988). Combustion and Flame 74: 53.

[9] P. Boivin, C. Jimenez, A.L. Sanchez, F.A. Williams. (2011). Proc. Combust. Inst. 33: 517.